**RESEARCH ARTICLE**

# QUANTUM CHEMICAL AND KINETIC PROPERTIES EVALUATION OF METHYLCHROMENO[2,3-C]PYRAZOL-3(2H)-ONE FOR ALUMINUM CORROSION INHIBITION IN $H_2SO_4$ MEDIUM

**Mougo Andre Tigori[1], Cisse M'bouille[1], Yeo Mamadou[2], Koffi Koffi Rodolphe[1] and Paulin Marius Niamien[3]**

1. Laboratoire des Sciences et Technologies de l'Environnement, UFR Environnement, Universite Jean Lorougnon Guede, BP 150 Daloa, Côte d'Ivoire.
2. Laboratoire de Thermodynamique et de Physico-Chimie du Milieu, UFR SFA, Universite Nangui Abrogoua, 02 B.P. 801 Abidjan 02.
3. Laboratoire de Constitution et de Reaction de la Matière, UFR SSMT, Universite Felix Houphouët-Boigny,22 BP 582 Abidjan 22, Côte d'Ivoire.

……………………………………………………………………………………………………....

## Manuscript Info

……………………..

## Abstract

……………………………………………………………………………………………

Despite the advantages of its use, aluminum remains vulnerable inacidi c environments. For this reason, this study evaluates the inhibition effic iency of 2 methylchromeno[2,3 c]pyrazol 3(2H) one (MCP) on aluminu m corrosion in 1 M sulfuric acid solution. Gravimetric measurements were combined with quantum chemical calculations. These calculations were based on Density Functional Theory(DFT) in basis set 6-31G(d,p) with B3LYP functional. The results show that inhibition efficiency increases with concentration and immersion time, while increasing temperature reduces inhibition efficiency. The increase in activation energy in the presence of 2-methylchromeno[2,3-c]pyrazol-3(2H)-one confirms the predominance of physisorption, corroborated by activation enthalpy and entropy values, indicating endothermic dissolution with increased disorder. Theoretical calculations reveal that MCP strong inhibition activity is linked to its ability to give up and accept electrons, favouring its adsorption by physico-chemical interactions dominated by electrostatic forces. Experimental and theoretical approaches converge perfectly, confirming that the inhibitor used is promising for the protection of aluminum in acidic media at low temperatures.
.

………………………………………………………………………………………………....

## Introduction:-

The industrial revolution, which continues to spread throughout the world, brings both benefits and negative impacts on the environment. Many industries use metals that are frequently exposed to aggressive environments, making them vulnerable to corrosion [1]. Metal corrosion, and aluminum corrosion in particular, is a major industrial and economic problem. Although aluminum is renowned for its natural resistance to oxidation, thanks to the spontaneous formation of a protective alumina layer, this barrier becomes unstable in highly acidic environments [2], particularly sulfuric acid. Under such conditions, aluminum undergoes accelerated degradation, resulting in

**Corresponding Author :** -Mougo Andre Tigori
**Address:-**Laboratoire des Sciences et Technologies de l'Environnement,UFR Environnement,Universite Jean Lorougnon Guede, BP 150 Daloa, Cote dIvoire.

material losses, reduced mechanical performance and higher maintenance costs [3]. To mitigate the deleterious effects of this degradation, the use of corrosion inhibitors has emerged as an effective, simple and economically viable strategy [4]. Among these, organic inhibitors are attracting growing interest due to their ability to adsorb onto metal surface via their heteroatoms (O, N, S) and conjugated π-systems, thus forming a protective film capable of reducing corrosive attack [5]. However, the choice of a high-performance inhibitor depends not only on its experimental efficacy. But also on an understanding of its electronic properties and kinetic behavior in relation to adsorption and dissolution mechanisms [6]. At present, organic inhibitors that are accessible and have low toxicity are preferred. In this context, Plant extracts and pharmaceutical compounds stand out for their low toxicity, conjugated structure and ability to interact effectively with metal surfaces [7]. Furthermore, in order to design more effective organic inhibitors, numerous studies have turned to quantum chemistry to establish precise correlations between the molecular properties of compounds and their inhibition capacity [8,9]. The molecular structure, including electronic distribution, electron density of active sites and frontier molecular orbitals, as well as various electronic parameters can be determined by theoretical calculations [10]. This information is used to predict the activity of an inhibitor on metal surface and to better understand adsorption mechanisms. It also permits to assess the relative efficacy of different compounds, paving the way for the rational design of more selective and effective inhibitors.

Within this framework, the main objective of the present study is to evaluate the anticorrosive properties of the compound 2-methylchromeno[2,3-c]pyrazol-3(2H)-one in the prevention of aluminum corrosion in 1 M sulfuric acid solution.

## Material and Methods:-
### Chemicals used:
The inhibitor used is 2-methylchromeno[2,3-c]pyrazol-3(2H)-one (MCP). It was synthesized and characterized by a team at Laboratory Organic Chemistry and Natural Synthesis of Felix Houphouet Boigny University, Cocody (Côte d'Ivoire). The molecular formula of this inhibitor is $C_{11}H_8N_2O_2$ with a molar mass M = 200.05 g/mol. Its molecular structure is shown in Figure 1.
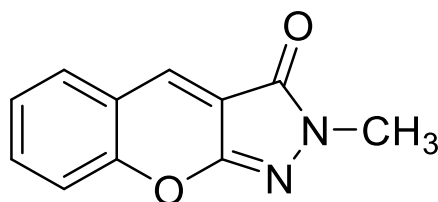


**Figure 1. Molecular structure of 2-methylchromeno[2,3-c]pyrazol-3(2H)-one (MCP)**

An acetone solution with purity P = 99.5%, density d = 0.79 and molar mass M = 58.08 g.mol$^{-1}$ was used to remove all traces of grease and native oxide from each aluminum sample. A sulfuric acid solution with purity P = 98%, density d = 1.84 and molar mass M = 98.08 g.mol$^{-1}$ was used to prepare a 1M concentration solution. This solution was used as a blank for all gravimetric tests.

### Gravimetric measurements:
Samples of 99%-pure aluminum in the form of cylindrical rods 10mm high and 25mm in diameter were polished with abrasive papers of successively finer grain sizes down to 800 grit, then thoroughly rinsed in distilled water. They were then washed in an acetone solution to remove all traces of oxide, before being dried in an oven at 80°C for 10 minutes. Each sample thus treated was weighed on a high-precision balance (± 0.1 mg), then immersed in 50 mL of a 1 M sulfuric acid solution, in the absence of inhibitor. The initial mass recorded ($m_1$) was then compared with that measured after a one-hour immersion in the sulfuric acid solution, this time containing the corrosion inhibitor. After this treatment, the samples were carefully rinsed, dried and weighed again to obtain the final mass ($m_2$). Mass loss was ($\Delta m = m_1 - m_2$) calculated by averaging three tests carried out under the same experimental conditions, with a margin error of ±0.3mg. To study the influence of immersion time we maintained the temperature at 298K and while keeping the same MCP concentrations, mass losses were evaluated for 4h, 6h, 8h and 24h. From these data, the average corrosion rate (W), the rate of coverage of the metal surface by the inhibitor (θ), and the inhibition efficiency (IE%) were calculated as a function of temperature and the concentration of inhibitor used. The following expressions were used to determine these corrosion parameters

$$W = \frac{m_1 - m_2}{S_e.t} = \frac{\Delta m}{S_e.t} \qquad (1)$$

$$IE(\%) = \frac{W_0 - W}{W_0} * 100 \qquad (2)$$

$W_0$ and $W$ (expressed in $g.cm^{-2}.h^{-1}$) are respectively the corrosion rate in the absence and presence of MCP, $S_e$ is the total surface area of aluminum sample and $t$ is the immersion time.

**Computational details:**
To establish a correlation between experimental data and MCP's quantum chemistry parameters, its geometry was first optimized using Gaussview 5.0 computer graphics software. This optimization was carried out using B3LYP correlation exchange functional, in 6-31G(d, p) basis set [11,12] (Figure 2). This basis set enabled precise geometry and electronic properties to be obtained for a wider range of organic compounds. Global molecular descriptor calculations were performed using Gaussian 09 software [13]. Thus, quantum chemical parameters such as highest occupied molecular orbital energy ($E_{HOMO}$), lowest unoccupied molecular orbital energy ($E_{LUMO}$), energy gap ($\Delta E$), dipole moment ($\mu$), ionization energy ($I$), electron, affinity ($A$), electronegativity ($\chi$), global hardness ($\eta$), global softness ($\sigma$), electrophylicity index ($\omega$), fraction of electrons transferred ($\Delta N$) andtotal energy ($E_T$) were calculated. The expressions below, derived from conceptual DFT, are used to calculate the quantum descriptors [14,15,16].

$$I = -E_{HOMO} \qquad (3)$$

$$A = -E_{LUMO} \qquad (4)$$

$$\Delta E = E_{LUMO} - E_{HOMO} \qquad (5)$$

$$\mu_P = \left(\frac{\partial E}{\partial N}\right)_{v(r)} = -\chi \qquad (6)$$

$$\chi = \frac{I+A}{2} \qquad (7)$$

$$\sigma = \frac{1}{\eta} = \frac{2}{I-A} \qquad (8)$$

$$\eta = \frac{I-A}{2} \qquad (9)$$

$$\omega = \frac{\mu_P^2}{2\eta} = \frac{(I+A)^2}{4(I-A)} \qquad (10)$$

$$\Delta N = \frac{\phi_{Al} - \chi_i}{2(\eta_{Al} + \eta_i)} \qquad (11)$$

For calculations the theoretical values of $\phi_{Al} = 4.28$ eV [17]and hardness $\eta_{Al} = 0$ [17] have been used for aluminum.
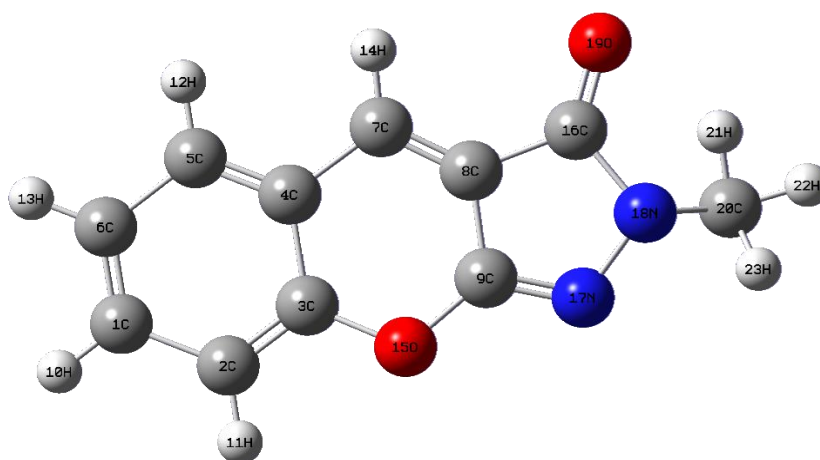


**Figure 2. Optimized structure of 2-methylchromeno[2,3-c]pyrazol-3(2H)-one**

## Results and Discussion:-

**Effect of temperature and concentration:**

To evaluate the influence of temperature and inhibitor concentration, the inhibition efficiency values obtained under different experimental conditions were plotted as a function of these two parameters (Figure 3). This representation illustrates the evolution of efficiency with respect to concentration at various temperatures and highlights the effect of temperature variation for a given concentration.
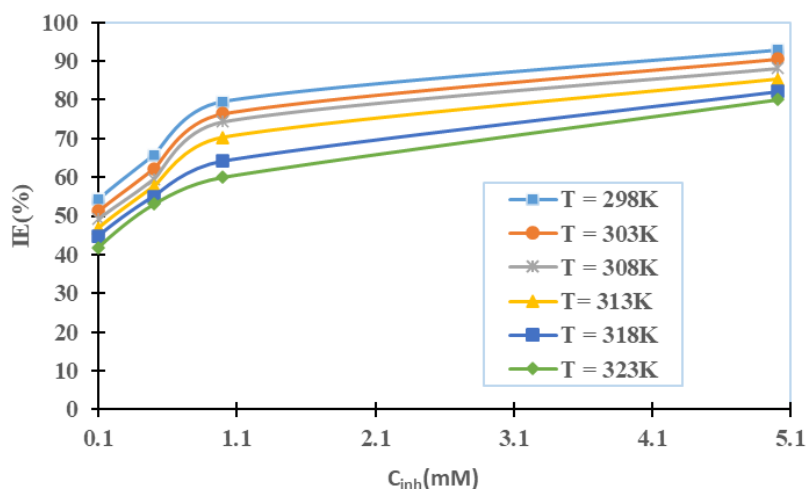


**Figure 3. Evolution of inhibition efficiency as a function of concentration and temperature**

The experimental curves show an upward trend in inhibition efficiency as a function of MCP concentration. Figure 3 examination shows clearly that the effectiveness of this compound increases with increasing concentration, while it tends to decrease with increasing temperature. The maximum value recorded is 92.87% at 298 K.

MCP inhibition action can be explained by the adsorption of its molecules onto aluminum surface. This adsorption limits the dissolution of the metal substrate and reduces its mass loss. The increase in inhibition efficiency with rising concentration results from the progressive coverage of the surface by inhibitor molecules. Heteroatoms (N, O) presence, combined with the aromatic character and the electron density of its $\pi$ systems, promotes the formation of a stable protective film. This film acts as a physical barrier, whose thickness and compactness increase proportionally with the MCP concentration, thereby hindering the corrosion process.

Conversely, higher temperatures lead to a decrease in inhibition efficiency. This reduction can be attributed to the partial desorption of adsorbed molecules or to the increased corrosive activity of the medium, which intensifies metal dissolution. As a result, the protective layer becomes progressively less effective, and the mass loss of aluminum increases.

**Immersion time effect:**

Figure 4 shows the evolution of inhibition efficiency as a function of immersion time.
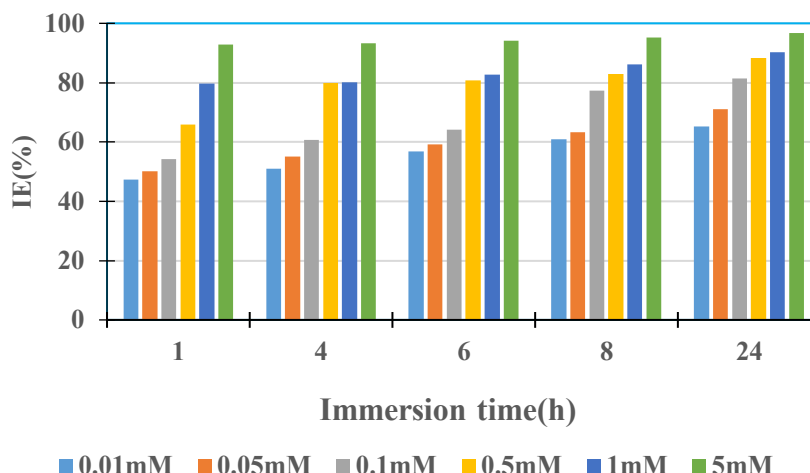
**Figure 4. Evolution of inhibition efficiency as a function of immersion time and concentration**

Figure 4 Analysis shows a progressive increase in inhibition efficiency with increasing MCP concentration and immersion time. These results indicate that the inhibition effect is greater at higher MCP concentrations and longer contact times with the metal surface. In particular, after 24 hours of immersion, the measured efficiency is slightly higher than that observed for shorter durations (1 h, 4 h, 6 h, and 8 h), suggesting that prolonged immersion promotes a completer and more stable adsorption of MCP molecules on aluminum surface. However, even a one-hour exposure is sufficient to reveal the molecule's inhibition properties significantly. All the observations highlight a progressive and reinforced attachment of MCP to metal substrate, leading to the formation of a protective layer that limits the corrosive attack of sulfuric medium. This behavior confirms the effectiveness of MCP as an aluminum corrosion inhibitor and underscores its ability to maintain protective action under prolonged exposure conditions.

**Activation parameters analysis:**
**Activation energy:**
The relationship between temperature and metal corrosion rate is based on the Arrhenius-type relationship. It is expressed as follows [20].

$$W = A\exp(-\frac{E_a}{RT}) \tag{12}$$

Using the relation $\log W = \log A - \frac{E_a}{2.3.R.T}$ , Figure 5 shows the evolution of $\log W$ as a function of $\frac{1}{T}$. Activation energy values are determined from the slopes of the straight lines obtained, and are given in Table 1.
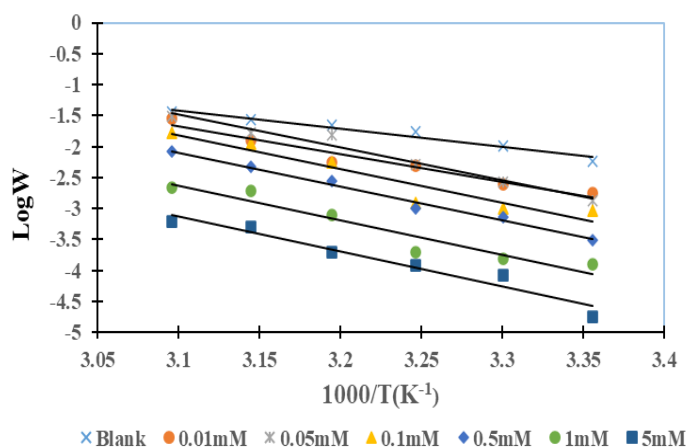


**Figure 5. $\log W$ versus $\frac{1}{T}$ .**

**Table 1. Activation Energy value**

| $C_{inh}$(mM) | Equations | $E_a$(kJmol$^{-1}$) |
|---|---|---|
| 0 | $logW = -2.954 * \frac{1}{T} + 7.7481$ | 56.60147584 |
| 0.01 | $logW = -4.5116 * \frac{1}{T} + 12.314$ | 86.44658714 |
| 0.05 | $logW = -5.3333 * \frac{1}{T} + 15.052$ | 102.191148 |
| 0.1 | $logW = -5.4824 * \frac{1}{T} + 15.183$ | 105.0480471 |
| 0.5 | $logW = -5.5071 * \frac{1}{T} + 14.98$ | 105.5213228 |
| 1 | $logW = -5.5514 * \frac{1}{T} + 14.58$ | 106.3701533 |
| 5 | $logW = -5.6562 * \frac{1}{T} + 14.408$ | 108.378222 |

The straight lines show that the corrosion rate increases as the temperature of the reaction medium rises. This rate is much higher in the absence (control) of the inhibitor. The values of activation energy ($E_a$)increase with increasing inhibitor concentration. This analysis shows that the presence of MCP increases activation energy required to dissolve the metal. The adsorption of its molecules onto metal surface requires significant energy, reflecting a blocking of active sites that requires a greater energy input. This rise in $E_a$accounts for the slowdown in the dissolution process in MCP presence, a slowdown that is all the more marked the higher the inhibitor concentration [20].

The activation energy values measured in the presence of MCP are significantly higher than those obtained in its absence. This suggests that MCP is adsorbed onto metal substrate via electrostatic bonds. However, these interactions, which are weak and sensitive to temperature variations, do not provide effective corrosion inhibition at high temperatures. Thus, the poor inhibiting performance observed at high temperatures is due to the physiosorbed nature of the interaction between the MCP and the metal surface [21].

**Enthalpy and entropy of Activation:**

Enthalpy variations($\Delta H_a^*$)and entropy ($\Delta S_a^*$)were determined from the alternative formula of Arrhenius equation:

$$log(\frac{W}{T}) = log(\frac{R}{\aleph.h}) + \frac{\Delta S_a^*}{2,3.R} - \frac{\Delta H_a^*}{2.3.R.T} \qquad (13)$$

Where A: Pre-exponential factor; W : Corrosion rate, R: Perfect gas constant; T: absolute temperature; $\aleph$ : Avogadro number; h : Planck's constant;

Figure 6 shows the evolution of $log(\frac{W}{T})$ depending on $\frac{1}{T}$. The slopes and intercepts of the lines obtained were used to determine these activation quantities. Table 2 shows the characteristics of the lines obtained and the values of $\Delta H_a^*$ et $\Delta S_a^*$.
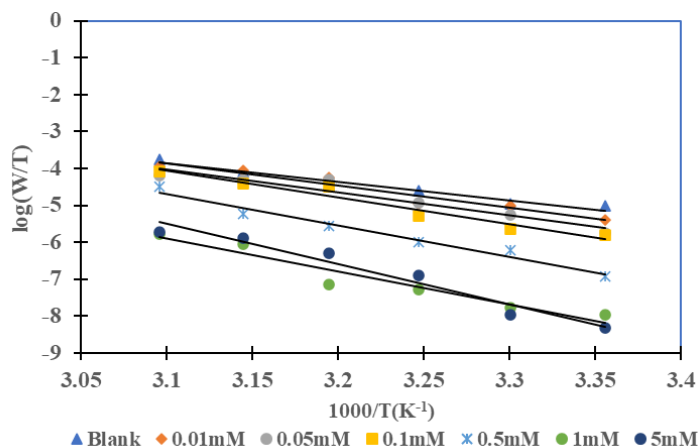


**Figure 6. $log(\frac{W}{T})$ versus $\frac{1}{T}$ .**

The values of activation enthalpy ($\Delta H_a^*$). are positive and increase with increasing MCP concentration. The positive enthalpy reflects the endothermic nature of aluminum dissolution process in sulfuric acid solution [22]. In addition, the high, positive values of activation entropy ($\Delta S_a^*$) indicate that the kinetically decisive step is associated more with a dissociation phenomenon than with an association mechanism [23,24]. This positive entropy reflects an increase in disorder during the transformation of reactants into the activated complex. This increased disorder results from the desorption of species initially attached to aluminum surface, progressively replaced by water molecules already present in the reaction medium.

**Tableau 2. Values ofenthalpy ($\Delta H_a^*$) and entropy ($\Delta S_a^*$)**

| $C_{inh}$(mM) | Equations | $\Delta H_a^*$(kJ. mol$^{-1}$) | $\Delta S_a^*$(J. mol$^{-1}$K$^{-1}$) |
|---|---|---|---|
| 0 | $\log W = -5.007 * \frac{1}{T} + 11.668$ | 95.93892672 | 25.795328 |
| 0.01 | $\log W = -5.9614 * \frac{1}{T} + 14.609$ | 114.2261469 | 82.074304 |
| 0.05 | $\log W = -6.2186 * \frac{1}{T} + 15.258$ | 119.1543459 | 94.493568 |
| 0.1 | $\log W = -7.1841 * \frac{1}{T} + 18.202$ | 137.6542527 | 150.829952 |
| 0.5 | $\log W = -8.5199 * \frac{1}{T} + 21.728$ | 163.2494631 | 218.303488 |
| 1 | $\log W = -8.9259 * \frac{1}{T} + 21.775$ | 171.0288129 | 219.20288 |
| 5 | $\log W = -10.978 * \frac{1}{T} + 28.54$ | 210.3490189 | 348.65792 |

**Quantum chemical properties of the inhibitor:**
**Global reactivity:**
The quantum chemical properties of the inhibitor are based on the global reactivity quantum chemical parameters. These parameters were calculated using DFT and are shown in Table 3.

**Table 3. Global reactivityparameters**

| Quantum descriptors of global reactivity | Values |
|---|---|
| $E_{HOMO}$ (eV) | -5.5474 |
| $E_{LUMO}$ (eV) | -2.6281 |
| Energy Gap $\Delta E$ (eV) | 2.9193 |
| dipole moment$\mu$ (D) | 3.5516 |
| ionization energyI (eV) | 5.5474 |
| Electron, affinityA (eV) | 2.6281 |
| Electronegativity$\chi$ (eV) | 4.0878 |
| Global hardness$\eta$ (eV) | 1.4597 |
| Global softness ($\sigma$) (eV)$^{-1}$ | 0.6851 |
| Fraction of electrons transferred$\Delta N$ | 0.0658 |
| Electrophylicity index$\omega$ | 5.7240 |
| Total energy $E_T$(Ha) | -683.6605 |

In light of previous work [25,26] the values obtained for highest occupied molecular orbital energy ($E_{HOMO}$) and that of lowest unoccupied molecular orbital energy ($E_{LUMO}$) are found to be high and low respectively. These characteristics suggest that the studied molecule exhibits a significant ability for electron transfer with aluminum, being capable of both donating and accepting electrons. This dual ability favors covalent bonds formation between inhibitor and metal, facilitating its adsorption onto surface and leading a protective film formation. This acts as an insulating barrier to aggressive environment. This observation confirms the link between the high inhibition efficiency recorded at low temperatures and the molecule's ability to act as both electron donor and electron acceptor.

Furthermore, energy gap ($\Delta E = E_{LUMO} - E_{HOMO}$) constitutes a key parameter of molecular reactivity: the smaller this gap, the more reactive [27,28]. Thus, the low value of $\Delta E$ obtained for MCP reflects a high reactivity, consistent with its experimentally demonstrated inhibition efficiency.

With regard to dipole moment ($\mu$), the literature is divided on its role in predicting inhibition efficiency [29,30]. Some authors note no clear correlation between $\mu$ and anticorrosive action, while others consider that a low value of the dipole moment would favor adsorption of the molecule and, consequently, its protective efficacy [31,32 ]. The results of the present study seem to agree with the latter hypothesis, suggesting that a reduced dipole moment facilitates the accumulation of MCP on metal surface and enhances its inhibition power.

A comparison of electronegativities shows that of aluminum (4.28 eV) is higher than that of MCP (4.0878 eV), resulting in a positive fraction of electrons transferred ($\Delta N$). This transfer of electrons from the molecule to metal helps compensate for the electron deficit caused by aggressive ions from sulfuric acid.

Finally, a study of electronic distributions of HOMO and LUMO orbitals (Figure 7) reveals that they are mainly located around nitrogen (N) and oxygen (O) atoms, as well as in aromatic regions. The mapping shows that the positive phase of the orbitals is represented by color red, while negative phase appears in green.

The red/green areas show HOMO and LUMO electronic distributions within the molecule. The electronic distributions of the highest occupied molecular orbital (HOMO) highlight localized areas on nitrogen (N) and oxygen (O) atoms, as well as on aromatic rings. This distribution suggests that these sites are the main centers of electron donation onto metal surface. Similarly, the regions associated with the lowest unoccupied molecular orbital (LUMO) also appear on aromatic rings and on the same heteroatoms, reflecting the molecule's ability to accept electrons from the metal and establish covalent bonds. These results indicate that interaction between MCP molecule and the metal surface occurs preferentially at sites enriched in $\pi$ electron density.
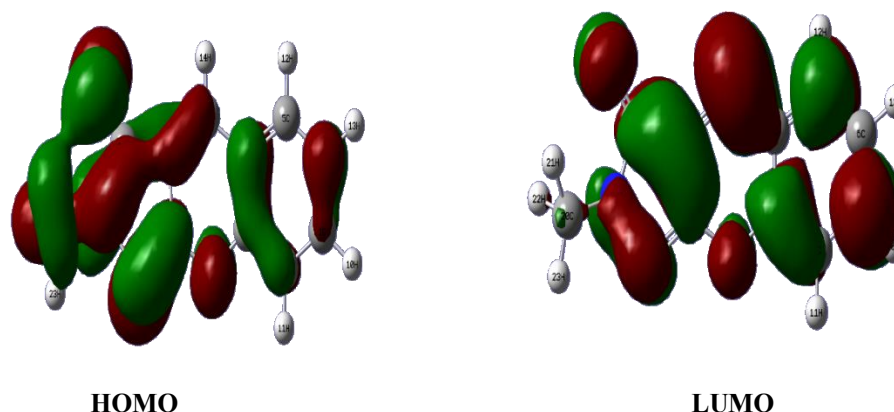


**HOMO**                          **LUMO**
**Figure 7. HOMO and LUMO Orbitals**

**Identifying sites of local reactivity:**
Active sites were identified using Fukui and dual descriptor functions. The following formulas are used to determine these local reactivity parameters [32-35]:
* Nucleophilic attack $f_k^+ = q_k(N+1) - q_k(N)$      (14)
* Electrophilic attack $f_k^- = q_k(N) - q_k(N-1)$      (15)
* Dual descriptor $\Delta f_k(r) = f_k^+ - f_k^-$          (16)
  Where $q_k(N+1)$, $q_k(N)$ et $q_k(N-1)$ are the electronic population of atomic sites k in $(N+1)$, N and $(N-1)$ electronic systems

The values of these local reactivity chemical quantum parameters are listed in Table 4.
These values include both positive and negative values. According to previous studies, the highest positive value of $f_k^+$ and $\Delta f_k(r)$ indicates the most likely site for nucleophilic attacks [34]. For the molecule studied, carbon C(20) is therefore the most likely site for nucleophilic attack. In this case, C(20) carbon is a zone ready to receive electrons from the metal. While a higher value $f_k^-$ and the lowest value of $\Delta f_k(r)$ identifies the most likely site for electrophilic attack. C(9) atom is then the most likely site for electrophilic attack. This site is the zone that supplies electrons to metal.

**Table 4. Mulliken atomic charges and local reactivity quantum parameters**

| Atom | $q_k(N+1)$ | $q_k(N)$ | $q_k(N-1)$ | $f_k^+$ | $f_k^-$ | $\Delta f_k(r)$ |
|---|---|---|---|---|---|---|
| 1  C | -0.007634 | -0.076945 | 0.143311 | 0.069311 | -0.220256 | 0.289567 |
| 2  C | 0.011242 | -0.159172 | -0.03122 | 0.170414 | -0.127952 | 0.298366 |
| 3  C | -0.005409 | 0.339114 | 0.04238 | -0.344523 | 0.296734 | -0.641257 |
| 4  C | 0.003203 | 0.074489 | -0.06016 | -0.071286 | 0.134649 | -0.205935 |
| 5  C | -0.005173 | -0.154381 | 0.192107 | 0.149208 | -0.346488 | 0.495696 |
| 6  C | 0.007202 | -0.088839 | -0.072796 | 0.096041 | -0.016043 | 0.112084 |
| 7  C | -0.011997 | -0.102503 | 0.396382 | 0.090506 | -0.498885 | 0.589391 |
| 8  C | -0.000342 | 0.015038 | 0.048092 | -0.01538 | -0.033054 | 0.017674 |
| **9  C** | 0.029219 | 0.553039 | 0.010143 | -0.52382 | **0.542896** | **-1.066716** |
| 10  H | 0.000275 | 0.108887 | -0.007338 | -0.108612 | 0.116225 | -0.224837 |
| 11  H | -0.000466 | 0.119505 | 0.000852 | -0.119971 | 0.118653 | -0.238624 |
| 12  H | 0.000222 | 0.109886 | -0.009021 | -0.109664 | 0.118907 | -0.228571 |
| 13  H | -0.000286 | 0.103358 | 0.002476 | -0.103644 | 0.100882 | -0.204526 |
| 14  H | 0.000451 | 0.135906 | -0.018103 | -0.135455 | 0.154009 | -0.289464 |
| 15  O | 0.01853 | -0.5595 | 0.013716 | 0.57803 | -0.573216 | 1.151246 |
| 16  C | 0.004862 | 0.558213 | 0.144803 | -0.553351 | 0.41341 | -0.966761 |
| 17  N | 0.020691 | -0.326793 | 0.096373 | 0.347484 | -0.423166 | 0.77065 |
| 18  N | 0.173387 | -0.371898 | -0.027181 | 0.545285 | -0.344717 | 0.890002 |
| 19  O | 0.040142 | -0.512522 | 0.11831 | 0,552664 | -0,630832 | 1,183496 |
| **20  C** | 0.758347 | -0.452087 | 0,042464 | **1.210434** | -0.494551 | **1.704985** |
| 21  H | -0.013917 | 0.20862 | -0.004673 | -0.222537 | 0.213293 | -0.43583 |
| 22  H | -0.00632 | 0.241832 | -0.018799 | -0.248152 | 0.260631 | -0.508783 |
| 23  H | -0.01623 | 0.236756 | -0.002119 | -0.252986 | 0.238875 | -0.491861 |

**Inhibition mechanism:**

MCP mechanism inhibition of aluminum corrosion in $H_2SO_4$ ,1M can be explained as follows. MCP compound is protonated in sulfuric acid solution, and the protonated species will be in equilibrium with its corresponding neutral phase according to the following equation:

$$2MCP + H_2SO_4 \rightleftarrows 2[MCPH]^+ + SO_4^{2-} \qquad (17)$$
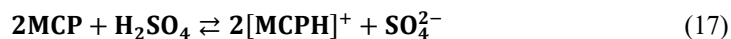
The protonated form of the inhibitor interacts with the negatively charged aluminum surface, due to the prior adsorption of sulfate ions ($SO_4^{2-}$) from sulfuric acid. This interaction promotes a protective film formation stabilized by electrostatic forces between the ionic species of inhibitor and sulfate ions, reflecting a physisorption mechanism. On the other hand, the inhibitor is also adsorbed by donor-acceptor interactions, involving the free doublets of heteroatoms as well as π-electrons of aromatic rings. This mode of interaction, associated with a charge transfer between molecule and metal, corresponds to a chemisorption process. The study of electronic parameters such as the number of electrons transferred ($\Delta N$), the energies $E_{HOMO}$, $E_{LUMO}$, as well as energy gap ($\Delta E$) confirms this second type of adsorption. The inhibition mechanism is summarized in Figure 8. The green line indicates chemisorption, while the red broken line shows the electrostatic interaction between the sulfate ion and the cationic form of MCP (physisorption).
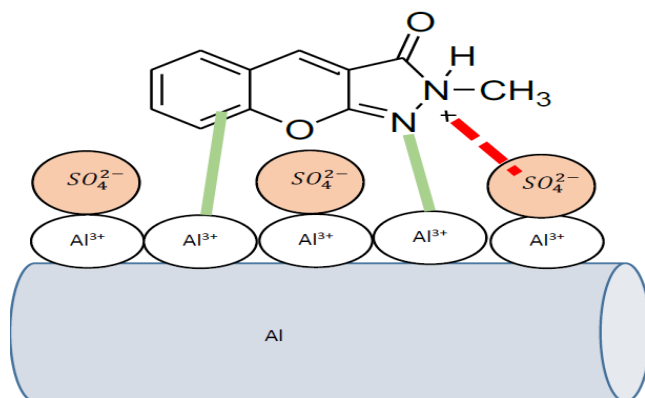
**Figure 8**. **Mechanism for inhibiting aluminum corrosion in $H_2SO_4$**

## Conclusions:-

The study carried out on 2-methylchromeno[2,3-c]pyrazol-3(2H)-one (MCP) highlighted its notable effectiveness as an aluminum corrosion inhibitor in a 1 M sulfuric acid medium.

Experimental results from gravimetric measurements showed that the inhibition efficiency of MCP increased with concentration and immersion time, reaching a maximum value of 92.87% at 298 K for 5 mM, while decreasing with increasing temperature.

Analysis of the activation parameters confirmed the predominance of a physisorption mechanism, supported by an endothermic process accompanied by an increase in disorder.

Quantum-chemical calculations carried out within DFT framework highlighted MCP's dual ability to give up and accept electrons, a property that favors its interaction with the metal surface via physico-chemical adsorption.

The identification of active sites showed that heteroatoms (O, N) and aromatic rings constitute the main centers of reactivity, playing a key role in the formation of a protective film on aluminum.

The convergence of experimental and theoretical data confirms that MCP is a promising organic inhibitor, capable of effectively limiting aluminum corrosion in acidic media at moderate temperatures. These results pave the way for the potential use of MCP in industrial applications.

## References:-

1. Nnabuk,O. E., Momoh-Yahaya, H. and Emeka, E. O. (2015). Theoretical and experimental studies on the corrosion inhibition potentials of some purines for aluminum in 0.1M HCl, Journal of Advanced Research,6(2):203-217.
2. Satoshi, H., Takuya M. and Minoru, O. (2025). Anion adsorption-induced charge separation at the alumina/aluminum interface. Corrosion Science,256,113150
3. Bochuan, T., Anqing, F., Lei, G., Yun, R., Junle, X.and Riadh, M.andWenpo, L.(2023). Insight into anti-corrosion mechanism of Dalbergia odorifera leaves extract as a biodegradable inhibitor for X70 steel in sulfuric acid medium. Industrial Crops and Products, 194:116106
4. Shawky, M. H., Elawady Y.A., Ahmed A.I.andBaghlaf A.O. (1979). Studies on the inhibition of aluminium dissolution by some hydrazine derivatives, Corrosion Science,19(12): 951-959
5. Rajeev, K. G., Manisha, M., Chandrabhan, V. and Quraishi, M.A.(2017).Aminoazobenzene and diaminoazobenzene functionalized graphene oxides as novel class of corrosion inhibitors for mild steel: Experimental and DFT studies,Materials Chemistry and Physics, 198: 360-373.
6. Chandrabhan, V., Eno, E. E., Quraishi, M. A.andChaudhery, M. H. (2021). Recent developments in sustainable corrosion inhibitors: design, performance and industrial scale applications, Materials Advances,2(12): 3806-3850).
7. Nomozov, A,Beknazarov, Kh.S, Normurodov, B.A., Misirov, Z.Kh., Yuldashova, S.G., Mukimova, G.J.,. Nabiev, D.A. andJumaeva, Z. (2025). Inhibition potential of Salsola oppositifolia extract as a greencorrosion inhibitor of mild steel in an acidic solution. International Journal of Corrosion and Scale Inhibition, 14(3):

1103–1115.

8.  Mustafa, R., Albayati, S. K., Necmi, D. Savaş, K., Riadh, M., Hassane, L., Rachid, S., Ismat, H. A., Majed, M. A.and Ill-Min, C.(2020).Synthesis, crystal structure, Hirshfeld surface analysis and DFT calculations of 2-[(2,3-dimethylphenyl)amino]-N'-[(E)-thiophen-2-ylmethylidene]benzohydrazide.Journal of Molecular Structure,1205:127654

9.  Suyu, J., Zhongheng, F., Guangxuan, S., Jiamin, P., Haiyan, G., Lingwei, M.and Dawei Z. (2025) Understanding and optimization of large language models for corrosion inhibition efficiency prediction. Corrosion Science,256,113217.

10. Adejoro, I.A., Akintayo, D.C.andIbeji C.U. (2016). The efficiency of chloroquine as corrosion inhibitor for aluminium in 1M HCl solution: Experimental and DFT study. Jordan Journal of Chemistry, 11(1): 38–49.

11. Lee, C., Yang W and Parr R.G. (1988). Development of the Colle-Salvetti Correlation-Energy Formula into a Functional of the Electron Density. Physical Review B, 37: 785–789.

12. Becke, A.D. (1993). Density-Functional Thermochemistry. III. The Role of Exact Exchange. Journal of Chemical Physics, 98: 1372–1377.

13. Frisch M.J., Trucks G.W., Schlegel H.B., Scuseria G.E., Robb M.A.and Cheeseman J.R. (2009). Gaussian 09.

14. Arafat, T., Omar, K. A., Ahmed, F., Ayman, M. M., Ahmed, Eldesoky M and Ahmed A. F. (2024). Effect of Adsorption and Interactions of New Triazole-Thione-Schiff Bases on the Corrosion Rate of Carbon Steel in 1 M HCl Solution: Theoretical and Experimental Evaluation ACS Omega , 2024 9 (6): 6761-6772.

15. Toghan, A., Fawzy, A., Alakhras, A.I., Alqarni, N.; Zaki, M.E.A., Sanad, M.M.S.and Farag, A.A.(2023) Experimental Exploration, RSM Modeling, and DFT/MD Simulations of the Anticorrosion Performance of Naturally Occurring Amygdalin and Raffinose for Aluminum in NaOH Solution. Coatings, 13: 704.

16. Mohamed, E. A., Altalhi, A. A., Amer, A., Negm, N. A., Azmy, E. A. M.and Farag, A. A. (2023). Two novel Schiff bases derived from 3-amino-1,2,4-triazole as corrosion inhibitors for carbon steel pipelines during acidizing treatment of oil wells: Laboratory and theoretical studies. Energy Sources, Part A: Recovery, Utilization, and Environmental Effects, 45(2): 3246–3265.

17. Pearson RG.(1988). Absolute Electronegativity and Hardness:application to Inorganic Chemistry, Inorganic Chemistry,27(4): 734-740.

18. Beda, R.H.B., Niamien, P.M., Avo Bile E.B., and Trokourey A. (2017). Inhibition of aluminum corrosion in 1.0 M HCl by caffeine: Experimental and DFT studies. Advances in Chemistry, Hindawi, Article ID 6975248.

19. Rokia T.H., Tigori M.A., Koffi A.A.and Niamien P.M. (2024). Exploring the anticorrosion performance of 2-(((4-chlorobenzyl)thiol)methyl)-1H-benzo[d]imidazole on aluminum in 1 M HNO3. Journal of Scientific Research, 16(3): 899–915.

20. Jmiai, A.,Tara,S, El Issami,M., Hilali,O., Jbara,L.and Bazzi. (2021). A new trend in corrosion protection of copper in acidic medium by using Jujube shell extract as an effective green and environmentally safe corrosion inhibitor: Experimental, quantum chemistry approach and Monte Carlo simulation study,Journal of Molecular Liquids. Journal of Molecular Liquids, 322, 114509.

21. Umoren, S.A., Obot, I.B.andEbenso, E.E. (2008). Corrosion inhibition of aluminium using exudate gum from Pachylobus edulis in the presence of halide ions in HCl. Journal of Chemistry, 5(2): 355.

22. Desai, P.S.and Desai, F.P. (2023). An overview of sustainable green inhibitors for aluminum in acid media. AIMS Environmental Science, 10(1): 33–62.

23. Desai, K.C., Desai, P.S.,Adarsh, Patel, M and Bhumika B. (2024). Caesalpinia crista seed is used as an eco-friendly inhibitor to prevent the corrosion of aluminium in hydrochloric acid solutions. Chemistry of Inorganic Materials, 4: 100067.

24. Yeo , M., Niamien, P. M., Bile E. B. A.andTrokourey, A. (2018). Thiamine hydrochloride as a potential inhibitor for aluminium corrosion in 1.0 M HCl: Mass Loss and DFT Studies. Journal of Computational Methods in Molecular Design, 8 :13–25.

25. Ammouchi, N., Allal, H., Belhocine, Y., Bettaz, S. and Zouaoui E. (2020). DFT computations and molecular dynamics investigations on conformers of some pyrazinamide derivatives as corrosion inhibitors for aluminum. Journal of Molecular Liquids, 300: 112309.

26. Eddy, N.O., Momoh-Yahaya, H.and Oguzie, E.E. (2015). Theoretical and experimental studies on the corrosion inhibition potentials of some purines for aluminum in 0.1 M HCl. Journal of Advanced Research, 6(2): 203–217.

27. Kumar, D., Jain, V .and Rai B. (2020). Imidazole derivatives as corrosion inhibitors for copper: A DFT and reactive force field study. Corrosion Science, 171: 108724.

28. Benhiba, F., Sebbar, N.K., Bourazmi, H., Belghiti, M.E., Hsissou, R.andHökelek T. (2021). Corrosion inhibition performance of 4-(prop-2-ynyl)-[1,4]-benzothiazin-3-one against mild steel in 1 M HCl solution:

Experimental and theoretical studies. International Journal of Hydrogen Energy, 46(51): 25800–25818.

29. Sahin, M., Gece G., Karei, F.andBilgic S. (2008). Experimental and theoretical study of the effect of some heterocyclic compounds on the corrosion of low carbon steel in 3.5% NaCl medium. Journal of Applied Electrochemistry, 38(1): 809–815.

30. Wazzan, N.A., Obot, I.B.and Kaya S. (2016). Theoretical modeling and molecular level insights into the corrosion inhibition activity of 2-amino-1,3,4-thiadiazole and its 5-alkyl derivatives. Journal of Molecular Liquids, 221: 579–602

31. Khaled K.F. (2008). Molecular simulation, quantum chemical calculations and electrochemical studies for inhibition of mild steel by triazoles. Electrochimica Acta, 53(9): 3484–3492.

32. Zhang, J., Li, W., Zuo X., Chen Y., Luo, W and Zhang Y. (2021). Combining experiment and theory researches to insight into anti-corrosion nature of a novel thiazole derivatives. Journal of the Taiwan Institute of Chemical Engineers, 122: 190–200.

33. Martínez-Araya, J.I. (2015). Why is the dual descriptor a more accurate local reactivity descriptor than Fukui functions. Journal of Mathematical Chemistry, 5: 451–465

34. Morell, C., Grand A.and Toro-Labbe A. (2005). New dual descriptor for chemical reactivity. Journal of Physical Chemistry A, 109: 205–212.

35. Damej, M., Kaya S., EL Ibrahimi, B., Lee, H.S., Molhi A. and Serdaroğlu G. (2021). The corrosion inhibition and adsorption behavior of mercaptobenzimidazole and bis-mercaptobenzimidazole on carbon steel in 1.0 M HCl: Experimental and computational insights. Surfaces and Interfaces, 24: 101095.